Textile-Reinforced Mortar versus FRP as Strengthening Material for Seismically Deficient RC Beam-Column Joints

Yousef A. Al-Salloum[1]; Nadeem A. Siddiqui[2]; Hussein M. Elsanadedy[3]; Aref A. Abadel[4]; and Mohammad A. Aqel[5]

Abstract: In this paper, efficiency and effectiveness of textile-reinforced mortars (TRM) on upgrading the shear strength and ductility of a seismically deficient exterior beam-column joint has been studied. The results are then compared with that of carbon fiber-reinforced polymer (CFRP) and glass fiber-reinforced polymer (GFRP)-strengthened joint specimens. Five as-built joint specimens were constructed with non-optimal design parameters (inadequate joint shear strength with no transverse reinforcement) representing an extreme case of preseismic code design construction practice of joints and encompassing the vast majority of existing beam-column connections. Out of these five as-built specimens, two specimens were used as baseline specimens (control specimens) and the other three were strengthened with TRM, CFRP, and GFRP sheets, respectively. All five subassemblages were subjected to quasi-static cyclic lateral load histories to provide the equivalent of severe earthquake damage. The response histories of control and strengthened specimens were then compared. The test results demonstrated that TRM can effectively improve both the shear strength and deformation capacity of seismically deficient beam-column joints to an extent that is comparable to the strength and ductility achieved by well-established CFRP, and GFRP-strengthening of joints. **DOI: 10.1061/(ASCE)CC.1943-5614.0000222.** *© 2011 American Society of Civil Engineers.*

CE Database subject headings: Beam columns; Joints; Fiber reinforced polymer; Seismic effects; Cyclic loads; Mortars.

Author keywords: Beam-column joints; TRM; GFRP; CFRP; Seismic; Strengthening; Cyclic loads.

Introduction

A majority of the pre-1970s constructed reinforced concrete (RC) frame buildings, existing across the world and within the Kingdom of Saudi Arabia, are shear deficient because they were constructed before the introduction of seismic codes for construction. Recent earthquakes have illustrated that inadequate shear reinforcement in the existing beam-column joints, especially exterior ones, is the prime cause of failure/collapse of moment resisting RC frame buildings. Hence, effective and economical rehabilitation techniques are needed to upgrade joint shear-resistance in existing structures. In the past, a variety of techniques have been employed to upgrade shear capacity and ductility of RC joints, with the most common being construction of RC or steel jackets. Plain or corrugated steel plates have also been tried. These techniques cause various difficulties in practical implementation at the joint, namely intensive labor, artful detailing, increased dimensions, corrosion protection, and special attachments. To overcome the difficulties associated with these techniques, recent research efforts have focused on the use of epoxy-bonded FRP sheets and/or TRM layers to enhance the shear capacity of poorly detailed joints.

There are several advantages of using FRP for rehabilitation of RC structures. These advantages are very well-reported in literature (Antonopoulos and Triantafillou 2003; Ghobarah and Said 2001, 2002; El-Amoury and Ghobarah 2002, Al-Salloum and Almusallam 2007). However, there are some drawbacks that require attention of FRP users. These drawbacks are (1) poor behavior of epoxy resins at temperatures above the glass transition temperature, (2) relatively high cost of epoxies, (3) hazards for the manual worker, (4) inability to apply FRP on wet surfaces or at low temperatures, (5) lack of vapor permeability, which may cause damage to the concrete structure, (6) incompatibility of epoxy resins and substrate materials, and (7) difficulty to conduct post-earthquake assessment of the damage suffered by the reinforced concrete behind (undamaged) FRP jackets. One possible solution to the previous problems would be the replacement of organic binders with inorganic ones, e.g., cement-based mortars and use of textile in place of fiber sheets.

Textiles comprise fabric meshes made of long woven, knitted, or even unwoven fiber roving in at least two (typically orthogonal) directions. Textile-reinforced mortar (TRM) was investigated in this study as a new method for strengthening and seismic retrofitting of concrete structures through jacketing. TRM jackets in this study consist of textile meshes made of carbon fibers roved in two directions and mortars, serving as binder, containing polymeric additives.

In the past, a number of excellent works have been reported on FRP-strengthened RC beam-column joints. Antonopoulos and Triantafillou (2003) conducted a comprehensive experimental program through two-thirds-scale testing of 18 exterior joints. Their study demonstrated the role of various parameters, e.g., area

[1]Professor, Dept. of Civil Engineering, King Saud Univ., Riyadh 11421, Saudi Arabia.

[2]Associate Professor, Dept. of Civil Engineering, King Saud Univ., Riyadh 11421, Saudi Arabia (corresponding author). E-mail: nadeem@ksu.edu.sa

[3]Assistant Professor, Dept. of Civil Engineering, King Saud Univ., Riyadh 11421, Saudi Arabia.

[4]MS Student, Dept. of Civil Engineering, King Saud Univ., Riyadh 11421, Saudi Arabia.

[5]Research Assistant, Dept. of Civil Engineering, King Saud Univ., Riyadh 11421, Saudi Arabia.

Note. This manuscript was submitted on November 2, 2010; approved on April 12, 2011; published online on April 14, 2011. Discussion period open until May 1, 2012; separate discussions must be submitted for individual papers. This paper is part of the ***Journal of Composites for Construction***, Vol. 15, No. 6, December 1, 2011. ©ASCE, ISSN 1090-0268/2011/6-920–933/$25.00.

Downloaded 01 Apr 2012 to 212.138.47.15. Redistribution subject to ASCE license or copyright. Visit http://www.ascelibrary.org

fraction of FRP and distribution of FRP, on shear strength of exterior joints. They also highlighted the importance of mechanical anchorages in limiting premature debonding. Ghobarah and Said (2001, 2002), El-Amoury and Ghobarah (2002), Al-Salloum and Almusallam (2007), Alsayed et al. (2010a, b), and Al-Salloum et al. (2011) developed effective selective rehabilitation schemes for R/C beam-column joints by using advanced composite materials. Mukherjee and Joshi (2005) experimentally studied the effect of FRP in improving shear strength and ductility of RC beam-column joints under simulated seismic forces. Ghobarah and El-Amoury (2005) developed effective rehabilitation systems to upgrade the resistance to bond-slip of the bottom steel bars anchored in the joint zone and to upgrade the shear resistance of beam-column joints. Antonopoulos and Triantafillou (2002), Gergely et al. (2000), and Almusallam and Al-Salloum (2007) presented analytical models for the prediction of shear capacity of the FRP-strengthened beam-column joints. Pampanin et al. (2007) carried out experimental and analytical investigations on CFRP retrofitted existing beam-column joint subassemblies and frame systems. Their experimental results provided very satisfactory confirmation of the viability and reliability of the adopted retrofit solution and of the proposed analytical procedure to predict the actual sequence of events. Karayannis and Sirkelis (2008) presented results of an experimental investigation on the behavior of critical external beam-column joints repaired and/or strengthened with a combination of epoxy resin injections and CFRP sheets. They concluded that the epoxy resin injections with the use of CFRP sheets leads to a significant improvement of the loading capcity, the energy absorption, and the ductility. Tsonos (2008) investigated experimentally and analytically the effectiveness of a reinforced concrete jacket and a high-strength fiber jacket for cases of postearthquake and preearthquake retrofitting of columns and beam-column joints. He also compared the effectiveness of the two jackets. Lee et al. (2010) proposed an effective rehabilitation strategy to enhance the strength and stiffness of the beam-column joint. They also proposed an analytical model to predict the column shear of the joints strengthened with CFRP. They employed a new optical noncontact technique, digital image correlation (DIC), to measure and observe the full strain field of the joint. Their experimental results showed that the beam-column joints strengthened with CFRP can increase structural stiffness, strength, and energy dissipation capacity. The proposed rehabilitation strategy was effective to increase the ductility of the joint and transform the failure mode to beam or delay the shear failure mode. Tsonos (2010) investigated the effectiveness and suitability of shotcrete and cast-in-place concrete as a means of retrofitting columns and beam-column joints in reinforced concrete frame structures to improve their shear and/or flexural performance. The use of four-sided and two-sided reinforced shotcrete or cast-in-place concrete jackets were investigated experimentally for the case of preearthquake retrofitting of columns and beam-column joints. Focus was placed on studying their lateral performance and on comparing the effectiveness of the reinforced shotcrete jackets with reference to the corresponding cast-in-place ones and that of the two-sided jackets with reference to the corresponding four-sided ones. All types of concrete jackets examined were found to be equally satisfactory in their ability to strengthen existing old frame structures. Di Ludovico et al. (2008) assessed the opportunities provided by the use of FRP for the seismic retrofit of existing RC structures by conducting tests on a full-scale three-story framed structure. Theoretical predictions were compared with the main experimental outcomes to assess the effectiveness of the proposed retrofit technique and validate the adopted design procedures. The experimental results confirmed the theoretical predictions, showing that the FRP retrofit allowed the structure to withstand a level of excitation in two directions, 1.5 times higher than that applied to the as-built structure, without exhibiting significant damage or structural deterioration. Balsamo et al. (2005) studied the effectiveness of CFRP composites for the seismic repair of RC structures by testing a full-scale dual system subjected to pseudodynamic tests in the ELSA laboratory. Their aim of the CFRP repair was to recover the structural properties that the frame had before the seismic actions. The repair was characterized by a selection of different fiber textures depending on the main mechanism controlling each component. The driving principles in the design of the CFRP repair and the outcomes of the experimental tests were presented. Comparisons between original and repaired structures were discussed in global and local performance. Engindeniz et al. (2008a) presented the performance of a full-scale reinforced concrete corner beam-column-slab specimen that was first severely damaged under bidirectional quasi-static loading then rehabilitated and retested. The specimen was built using the pre-1970s construction practices including the use of low-strength materials (21 MPa, Grade 40 reinforcing bars) and deficiencies in reinforcement detailing. The results indicated that even a severely damaged corner joint can be effectively rehabilitated by using CFRP to achieve a ductile beam failure mechanism. Engindeniz et al. (2008b) experimentally investigated the adequacy of corner beam-column joints in pre-1970 reinforced concrete buildings and determined the efficiency of CFRP composites for both pre- and postearthquake retrofit of such joints. Pantelides et al. (2008) experimentally studied the use of externally applied CFRP jackets for seismic rehabilitation of reinforced concrete interior beam-column joints, which were designed for gravity loads. The joints had steel reinforcement details that were inadequate by current seismic codes in joint shear capacity attributed to the absence of transverse steel hoops and bond capacity of beam bottom steel reinforcing bars at the joint. Lap splicing of beam bottom steel reinforcement at the joint by using externally applied longitudinal CFRP composite laminates was investigated. Improvement of joint shear capacity by using diagonal CFRP composite laminates was employed as another strengthening scheme. The test results indicated that CFRP jacketing is an effective rehabilitation measure for improving the seismic performance of existing beam-column joints with inadequate seismic details in increased joint shear strength and inelastic rotation capacity. They also found that CFRP laminates are effective rehabilitation measures for overcoming problems associated with beam bottom steel bars that have inadequate embedment into the beam-column joints.

The above review of the literature shows that substantial research has been conducted on the adequacy of FRP composites as a strengthening material for seismically deficient beam-column joints. However, very limited research is available on the use of TRM as a strengthening material for concrete structures, including RC beam-column joints. Triantafillou and Papanicolaou (2005) were among the early researchers to study the comparison between TRMs, and FRPs as shear strengthening materials for concrete structures and/or seismic retrofitting of concrete structures. The experimental investigations carried out provided a better understanding on the effectiveness of TRM versus FRP jackets in terms of increasing (1) the axial capacity of concrete through confinement and (2) the load-carrying capacity of shear-critical reinforced concrete flexural members. From the results obtained, they illustrated that the proposed TRM-strengthening technique is a viable alternative to the already successful FRP strengthening technique. Papanicolaou et al. (2007) experimentally investigated effectiveness of TRM overlays to strengthen masonry walls subjected to in-plane cyclic loading. From the results obtained, they observed that the use of TRMs is very promising for the structural upgrading of masonry structures subjected to in-plan seismic

Downloaded 01 Apr 2012 to 212.138.47.15. Redistribution subject to ASCE license or copyright. Visit http://www.ascelibrary.org

loading. Triantafillou et al. (2006) explored the application of TRMs as a means of increasing the axial capacity of concrete through confinement. They concluded that the textile-mortar jacketing provides a substantial increase in compressive strength and deformability, and this gain is higher as the number of confining layers increases and depends on the tensile strength of the mortar. Al-Jamous et al. (2006) studied the columns reinforced with textile layers circumferentially. They found that textile reinforcement improves the confinement significantly, and thus, the load bearing capacity of the columns under compressive stress increases. Triantafillou and Papanicolaou (2006) investigated that the TRM can be applied to increase the shear resistance of reinforced concrete members. It was concluded that textile-mortar jacketing provides substantial gain in shear resistance, and this gain is higher as the number of layers increases, and depending on the number of layers, it is sufficient to transform shear-type failure to flexural failure. In their study, TRM jackets were provided either by conventional wrapping of fabrics or by helically applied strips. Both systems resulted in excellent results in increasing the shear resistance. However, compared with their resin impregnated counterparts, mortar-impregnated textiles resulted in reduced effectiveness. They also derived a simplified truss analogy on the basis of a semiempirical model for prediction of shear resistance of reinforced concrete members strengthened with TRM jackets. The results of their study illustrate that TRM jacketing is an extremely promising solution for increasing the shear resistance of reinforced concrete members. Wu and Sun (2005) developed a cement-based composite thin fiber sheet for structural retrofit of concrete structural members. Retrofit efficiency of epoxy-based and cement-based thin fiber sheets was compared. They observed that the compressive and flexural strength of concrete can be significantly improved by using external FRC wraps. Also, the ductility of the retrofitted concrete was increased significantly. Kurtz and Balaguru (2001) studied beams after they were strengthened with carbon fiber sheets that were bonded with an inorganic matrix. This experimental study simulates an earlier study in which beams were strengthened in the same way by using an organic matrix. Strength, stiffness, ductility, failure pattern, and the cracking of beams strengthened with the two systems were compared. The results indicate that the inorganic matrix is as effective in increasing the strength and stiffness of reinforced concrete beams as the organic matrix, with a minor reduction in ductility. The failure mechanism changed from sheet delamination for the organic system to sheet rupture for the inorganic system. This change in mechanism was attributed to the brittleness of the inorganic matrix that results in a crack formation in the composite and a development of strain along the interface of the composite and concrete. Basalo et al. (2009) experimentally studied the confinement of concrete columns by using fiber-reinforced cementious matrix. They observed that the composite systems of fiber-reinforced cementious matrix increases both the strength and deformability of concrete cylinders.

The previous review of the literature clearly indicates that although there is considerable research on the use of TRM as strengthening material for concrete structural members and/or seismic retrofitting of concrete elements, work on TRM-strengthened beams-columns joints is very limited. In fact, the authors could not find any significant work on TRM-strengthened beam-column joints in the approachable references. Keeping this scope in view, authors have studied effectiveness and efficiency of TRM on the strengthening of beam-column joints to demonstrate that TRM-upgrading can effectively improve both the shear strength and ductility of seismically deficient beam-column joints to an extent that is comparable to the strength and deformability achieved by well-established CFRP- and GFRP-strengthening of joints.

Experimental Program

Test Matrix

One of the main objectives of the present study was to conduct an experimental program to evaluate seismic performance of a TRM-strengthened beam-column joint specimen and compare its performance with CFRP- and GFRP-upgraded beam-column exterior joint specimens. To accomplish this, five reinforced concrete as-built specimens (Fig. 1) were cast with the reinforcement details, as shown in Fig. 2. The nomenclature used for various specimens is shown in Table 1. In finding out the size of these specimens, a prototype member size was first chosen, and then a crude analysis was carried out to come up with the most reasonable scale for the test specimens that comply with the available testing facility and equipment. Half-scale beam-column joints were found to be the most convenient. The dimensions and details of prototype and half-scale as-built test specimens are shown in Figs. 1 and 2.

Material Properties

Concrete and Steel

For the construction of beam-column joint specimens, the concrete was obtained from a local ready-mix concrete company with a target compressive strength of 30 MPa. Upon arrival, the slump was measured as 105 mm, and six cylinders (150 × 300 mm) were cast to determine the 28-days compressive strength f'_c from the batch. The average compressive strength of concrete after 28 days of curing is shown in Table 2. To determine the actual characteristics of the reinforcing steel, the samples of steel used were tested in accordance with ASTM A370 (ASTM 2011). Three specimens of steel bars were tested by using an INSTRON tensile testing machine with hydraulic grips. Each specimen was subjected to a gradually increasing uniaxial load until failure took place. The average yield strength of three specimens is reported in Table 2. Stirrups were made of mild steel with an average yield stress equal to 260 MPa.

Carbon and Glass FRP System

The properties of composite materials are dependent on the individual components properties, the manufacturing technique, and the quality control of the production process. In the present study, glass and carbon FRP sheets supplied by FYFE Company were employed for the strengthening of beam-column joint specimens.

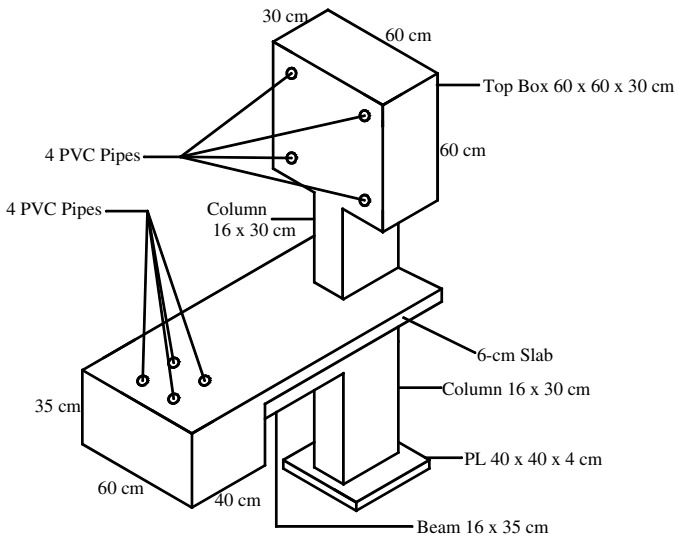

Fig. 1. Dimensions of exterior as-built joint specimen

Downloaded 01 Apr 2012 to 212.138.47.15. Redistribution subject to ASCE license or copyright. Visit http://www.ascelibrary.org

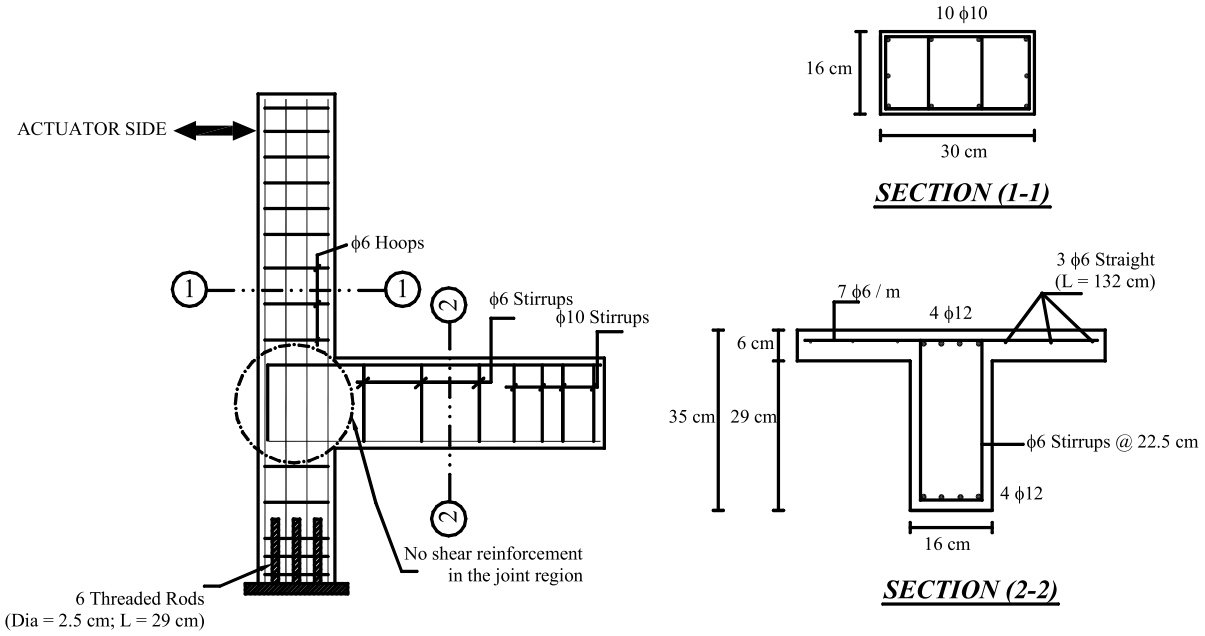

Fig. 2. Reinforcement details of the as-built specimen

Table 1. Nomenclature for Test Specimens

Group number	Specimen designation	The test conditions and retrofit schemes
Control specimens	ECON1	First as-built control specimen
	ECON2	Second as-built control specimen
Strengthened specimens	ECTRM	Strengthened specimen, obtained by strengthening the as-built specimen by using two layers of carbon textile-reinforced mortar CTRM
	ECFRP	Strengthened specimen, obtained by strengthening the as-built specimen by using single layer of CFRP sheets
	EGFRP	Strengthened specimen, obtained by strengthening the as-built specimen by using two layers of GFRP sheets

The coupon samples were cut from the sheets to determine the average mechanical properties of the sheets. The average coupon test results of the carbon and glass FRP system are shown in Table 2.

TRM Materials

Textile-reinforced mortar consist primarily of two materials: textile and mortar. Success of rehabilitation using TRM is very much dependent on the properties of these two constituents of TRM. The following subheadings provide details of the tests that were conducted on textile and mortar to evaluate their properties to have their confident use in beam-column joint strengthening.

Textile The outline of the jackets was marked on specimens, and the textile was cut to the required length. The textile contained an equal quantity of high-strength carbon fiber roving in each direction. They were simply placed on top of the others and bonded on a secondary polypropylene line, as shown in Fig. 3. To obtain the mechanical properties of textile used, four coupons of textile were tested in tension. Fig. 4 shows textile coupons under the test. Fig. 4 shows the typical dimensions of textile used in this study. Each roving was 3.93 mm wide, and the clear spacing between the roving was 10 mm. The nominal thickness of each layer was 0.4 mm. The coupon tests showed that guaranteed tensile strength of carbon fiber textile is equal to 777 MPa with an average strain of 0.0095 and modulus of elasticity equal to 82.33 GPa. The details of textile properties are summarized in Table 2.

Mortar In the present study, a commercial polymer-modified mortar (from SikaRep) was used to use as the mortar in TRM strengthening (Fig. 5). In the following subsection, the procedure adopted for the determination of the compressive and the tensile strengths of mortar has been presented.

Compressive Strength of Mortar To prepare the mortar for the compressive strength test, 16–18% of drinking quality water (by weight of dry powder) was put in a dry bowl; mortar was added, and then it was mixed from 3 to 5 min until homogeneous mixture was obtained. Molding of the specimens was then done by placing a layer of mortar about 25 mm in thickness in the cube compartments. Each layer in each cube compartment was tamped 32 times within 10 s in four rounds. After tamping of the first layer in all the cube compartments, the second layer was introduced and tamped in the same manner as previously mentioned. Finally, the top surface of the cube compartment was smoothed off with one stroke of the trowel. The specimens were air dried for one day and were demolded; the specimens were then kept for curing under lab conditions for 28 days. Standard compressive strength tests as per ASTM C109 (2002) at 7 and 28 days were conducted and presented in Table 3.

Tensile Strength of Mortar To determine the tensile strength of mortars, standard Briquette specimens were prepared having inside faces and a thickness at the waistline of the briquette mold of 25 mm. Briquette specimens for each mortar type using the same amount of water as determined for compressive strength were

Downloaded 01 Apr 2012 to 212.138.47.15. Redistribution subject to ASCE license or copyright. Visit http://www.ascelibrary.org

Table 2. Material Properties of Specimens

Parameter	Properties
Concrete and steel	
Average concrete strength, f'_c (MPa)	33.4
Average yield strength of steel, f_y (MPa)	510
CFRP composite system (Tyfo SCH-41S)	
Type of FRP	Unidirectional CFRP sheet
Elastic modulus in primary fibers direction	77.3×10^3 MPa
Elastic modulus of CFRP 90° to primary fibers	40.6 MPa
Fracture strain	1.1%
Ultimate tensile strength	846 MPa
Thickness per layer, t_f	1.0 mm
GFRP composite system (Tyfo SEH-51A)	
Type of FRP	Unidirectional GFRP sheet
Elastic modulus in primary fibers direction	28.9×10^3 MPa
Elastic modulus of GFRP 90° to primary fibers	25.8 MPa
Fracture strain	1.6%
Ultimate tensile strength	464 MPa
Thickness per layer, t_f	1.3 mm
Carbon textile fiber	
Type of textile	Carbon fiber
Elastic modulus per one textile	82.33 GPa
Fracture strain	0.95%
Ultimate tensile strength per one textile	777 MPa
Thickness per one textile, t_f	0.4 mm
Width per one textile	3.93 mm

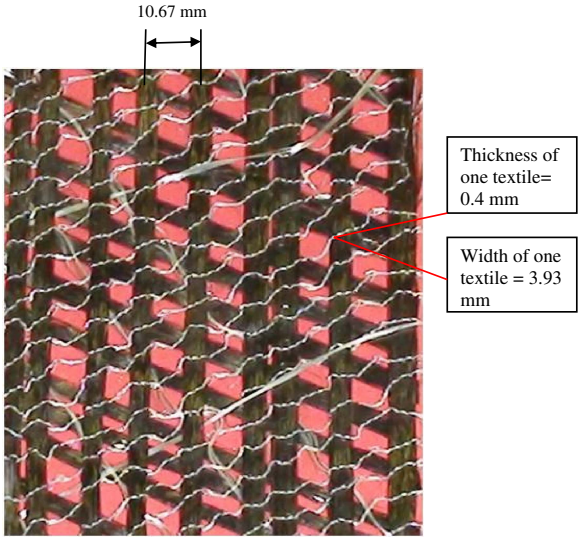

Fig. 3. Typical textile used in the present study

Fig. 4. Textile coupon under test (image by the authors)

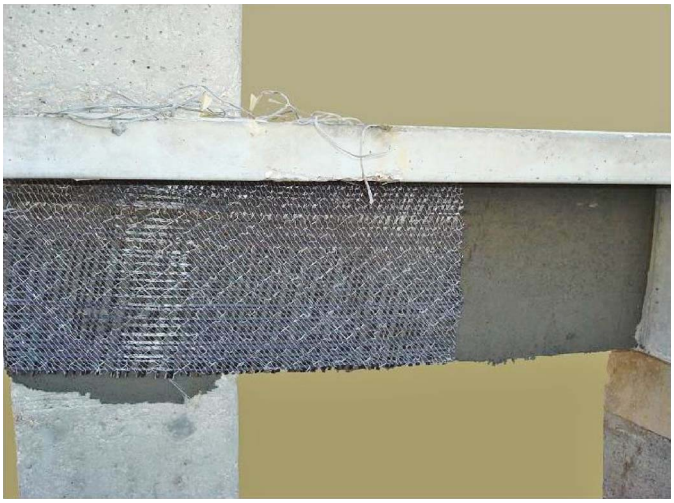

Fig. 5. Specimen during TRM strengthening (image by the authors)

prepared in accordance with ASTM C190-85 (1985). A thin film of oil was coated on the inside surfaces of the Briquette molds and placed on base plates. The molds were filled heaping full of mortar without any compacting. The mortars were pressed in firmly with the thumbs, applying a force 12 times to each Briquette. Additional mortar was added above the molds and smoothed off with a trowel. Other oiled metal plates were placed on top of each mold; bottom and top plates were held together and turned over. The procedure of adding additional mortar above the molds was repeated, pressed 12 times with thumbs, and smoothed off with a trowel. The specimens were air dried for one day. After one day of air drying, the specimens were demolded and kept for curing under lab conditions. Before testing, each Briquette was wiped to a surface-dry condition, and any loose sand grains from the surfaces were removed. Standard tensile tests as per ASTM C190-85 (1985) at 3, 7, and 28 days were conducted and presented in Table 3.

Design Procedure of the TRM, CFRP and GFRP Application

The design approach was based on providing fiber reinforcement to replace the missing joint shear reinforcement and the inadequately detailed steel bars. For this purpose, the specimen was externally bonded with a single layer of CFRP sheets to the joint, beam, and

Downloaded 01 Apr 2012 to 212.138.47.15. Redistribution subject to ASCE license or copyright. Visit http://www.ascelibrary.org

Table 3. Results of the Tensile and Compressive Strength of Tested Mortars

Physical property	Curing age (days)	Specimens 1	2	3	4	Average
Compressive strength (MPa)	7	37.32	34.04	35.88	36.4	35.91
	28	51.5	52.1	50.9	54.1	52.2
Tensile strength (MPa)	3	2.4	2.1	2.4	2.3	2.3
	7	2.8	2.9	3.8	—	3.16
	28	4.46	4.30	4.33	4.51	4.4

part of the column regions with the orientation of primary fibers, as shown by horizontal and vertical lines in Figs. 6 and 7. Figs. 6 and 7 show details of CFRP, GFRP, and TRM layup. To estimate the number of layers, the design procedure available in El-Amoury and Ghobarah (2002) was adopted. A single layer CFRP or double layer GFRP sheet was found adequate in upgrading the joint shear resistance of as-built joint specimens. Because no design procedure is available for the design of TRM-strengthened beam-column joints, the same procedure, as given in El-Amoury and Ghobarah (2002) for FRP-strengthened beam-column joints, was followed after calculating the equivalent cross sectional area of textiles, as shown subsequently. The number of layers was then estimated following the same calculation as followed for the FRP sheets. The desired number of textile layers was more than 2. However, because

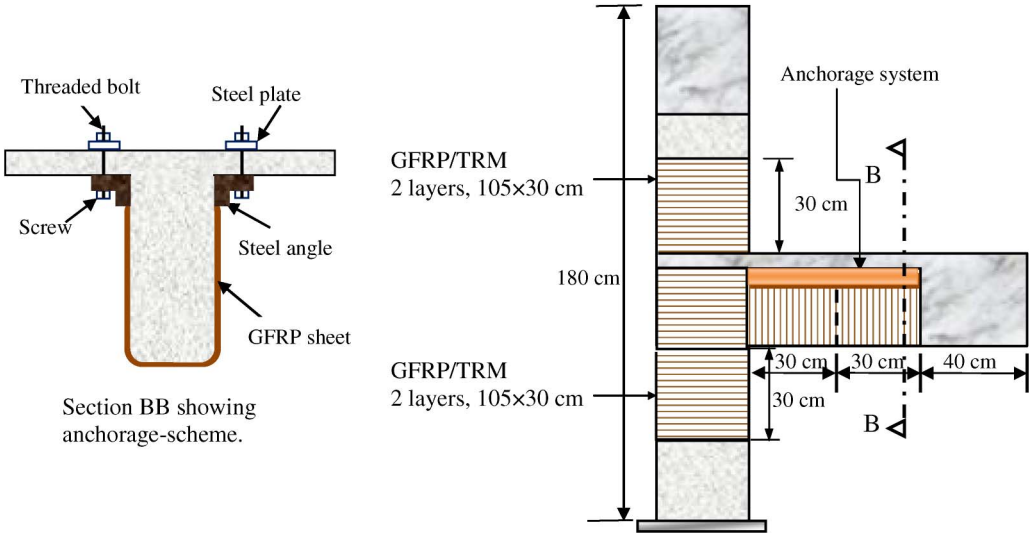

Fig. 6. Schematic representation of GFRP and TRM scheme applied to as-built exterior joint

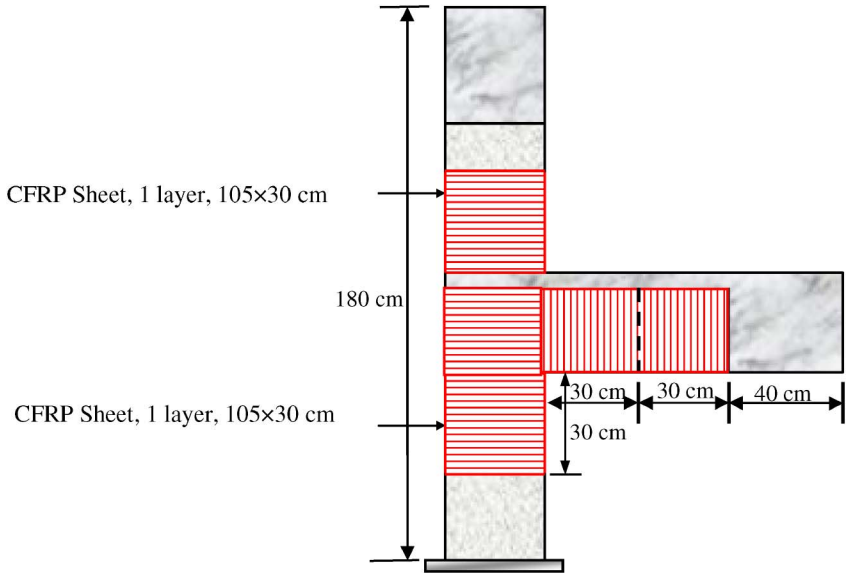

Fig. 7. Schematic representation of CFRP scheme applied to as-built exterior joint

Downloaded 01 Apr 2012 to 212.138.47.15. Redistribution subject to ASCE license or copyright. Visit http://www.ascelibrary.org

the present investigation was based on textile-reinforced mortar and not the textile alone, only two layers of TRM layers were selected for the present study.

To compare the cross sectional areas of strengthening materials, the values of thicknesses and widths of FRP sheets, given in Table 2, were employed to calculate their cross sectional areas in 1.00 m width of the FRP sheet. The results are 1,000 and 1,300 mm^2 for CFRP and GFRP sheets, respectively. For textile fibers of TRM, using the thickness (0.4 mm) and width (3.93 mm) of each textile fiber, as shown in Fig. 3 and Table 2, the cross-sectional area of each textile fiber was obtained. Then, by using the distance between the two consecutive textile fibers (10.67 mm), the area of textile cross section available to carry the tension in a 1 m width of TRM was calculated. This area of cross section was obtained as 147.3 mm^2/m width.

Strengthening of Specimen by Using TRM

After the specimen was cured and ready to be tested, the surface of the beam-column region, was grinded manually, and then, sandblasting was done, enabling it to develop a sound bond between the concrete and strengthening material. To strengthen the specimen by using external bonding of textiles with polymer modified cementitious mortars (TRM), the joint and beam were wrapped with *U*-shaped carbon textile layers. The ends of impregnated textiles with mortar layers were anchored by using a system of steel angles tied to steel plates through threaded rods driven through the concrete slab, as shown in Fig. 6. A part of the column regions was also wrapped, as shown in Fig. 6. The bolted plates (anchorage) allow the textile fibers to develop to their full capacity. The mortar was applied in approximately 2 mm thick layers. After the application of the first mortar layer on the (dampened) mortar surface, another layer of textile was applied and pressed slightly into the mortar, which protruded through all the perforations between the rovings. The next mortar layer covered the textile completely, and the operation was repeated until the required number of textile layers was applied and covered by the mortar. The specimen was cured by using wet burlaps for approximately 28 days. The bonding of jackets took place at a concrete age of 28 days.

Strengthening of Specimens by Using Carbon and Glass FRP Sheets

The two as-built specimens were strengthened using epoxy-bonded GFRP and CFRP sheets, respectively. The epoxy system used for external bonding of FRP sheets to the concrete surface consists of a two-component epoxy matrix material. The first component is resin, and the other component is hardener. The epoxy mix ratio contains 100 parts of resin to 42.0 parts of hardener by volume or 100 parts of resin and 34.5 parts of hardener by weight. The resin and the hardener were mixed thoroughly by using a mixing drill for at least 5 min. As shown in Figs. 6 and 7, GFRP and CFRP sheets were epoxy bonded to joint, beam and part of the column regions. For GFRP strengthening, two layers of unidirectional GFRP were used, whereas for CFRP strengthening, a single layer of CFRP sheet was used. From the strength point of view, two layers of GFRP sheets are equivalent to one layer of CFRP sheets. The orientation of primary fibers was maintained, as shown by horizontal and vertical lines in Figs. 6 and 7. In GFRP strengthening, mechanical anchorages were used in the beam region to prevent any possible debonding and to allow the fibers to develop to their full capacity. To apply mechanical anchorage system, three holes were drilled on either side of the extended epoxy-bonded GFRP-upgraded beam to the slab. One bolt was passed through each hole, and it was tightened effectively at the ends by using flat steel plates, as shown in Fig. 6. In case of CFRP-strengthened specimen (Fig. 7), the mechanical anchorage system was not used because debonding was not expected in this specimen because of the strong bond between CFRP sheets and the concrete surface. Figs. 6 and 7 illustrate the GFRP and CFRP schemes applied to as-built joint specimens.

Test Setup

The previous specimens (i.e., as-built control, CFRP, GFRP and TRM strengthened) were tested by using the testing apparatus designed and installed in the Structural Test Hall, Department of Civil Engineering, King Saud University, Saudi Arabia. To apply the simulated seismic-type cyclic load on the specimen, a 500-kN servocontrolled hydraulic actuator was connected to a reaction steel frame, which stands on a strong concrete floor. Figs. 8 and 9 show the details of the experimental setup. In the test setup, the bottom of the column surface was attached to a base pivot by using four high-strength threaded rods. The base pivot, in turn, was fastened to a strong steel I-beam. The latter was posttensioned to the lab floor by using high-strength posttensioning rods. The rigid end of the concrete beam was tied to a rigid link through a steel pivot.

Instrumentation

The joint specimens were instrumented with several measuring instruments. The details of the instrumentation layout are illustrated in Fig. 10. Four string potentiometers were affixed along the face of the column to measure lateral deflection at different locations along the column height. In addition, two string potentiometers were positioned along the surface of the concrete beam to measure its vertical deflection at different locations. To measure the joint rotation at the beam-column interface, four inclinometers were attached to the concrete surface, as shown in Fig. 10. Two linear variable displacement transducers were placed diagonally at the panel zone to assess the joint shear distortion during the experiment.

Internal strain gages were used to measure the strain of the longitudinal steel bars and transverse stirrups for both beam and column (Fig. 11). Just before the exterior specimen was put up for testing, a constant axial load was applied at the top of the column by posttensioning two threaded rods with a pair of hydraulic jacks mounted at the top of the column using rigid steel beam assembly, as shown in Fig. 8. In the present study, it was taken as 20% of the column axial load capacity and maintained constantly throughout the test.

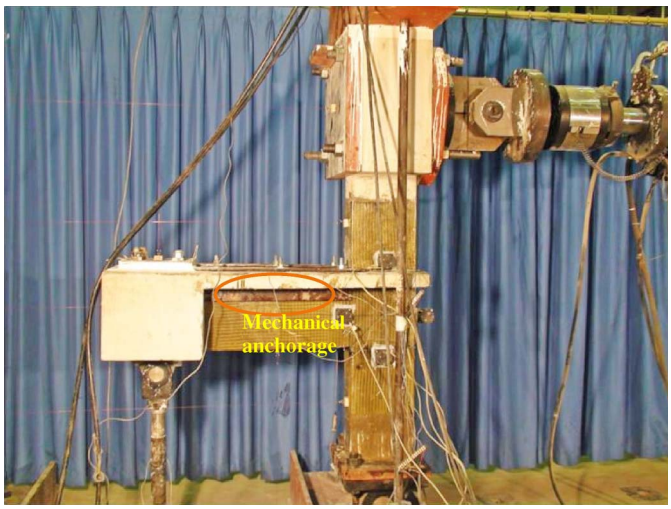

Fig. 8. Photo showing GFRP scheme applied to as-built exterior joint (image by the authors)

Downloaded 01 Apr 2012 to 212.138.47.15. Redistribution subject to ASCE license or copyright. Visit http://www.ascelibrary.org

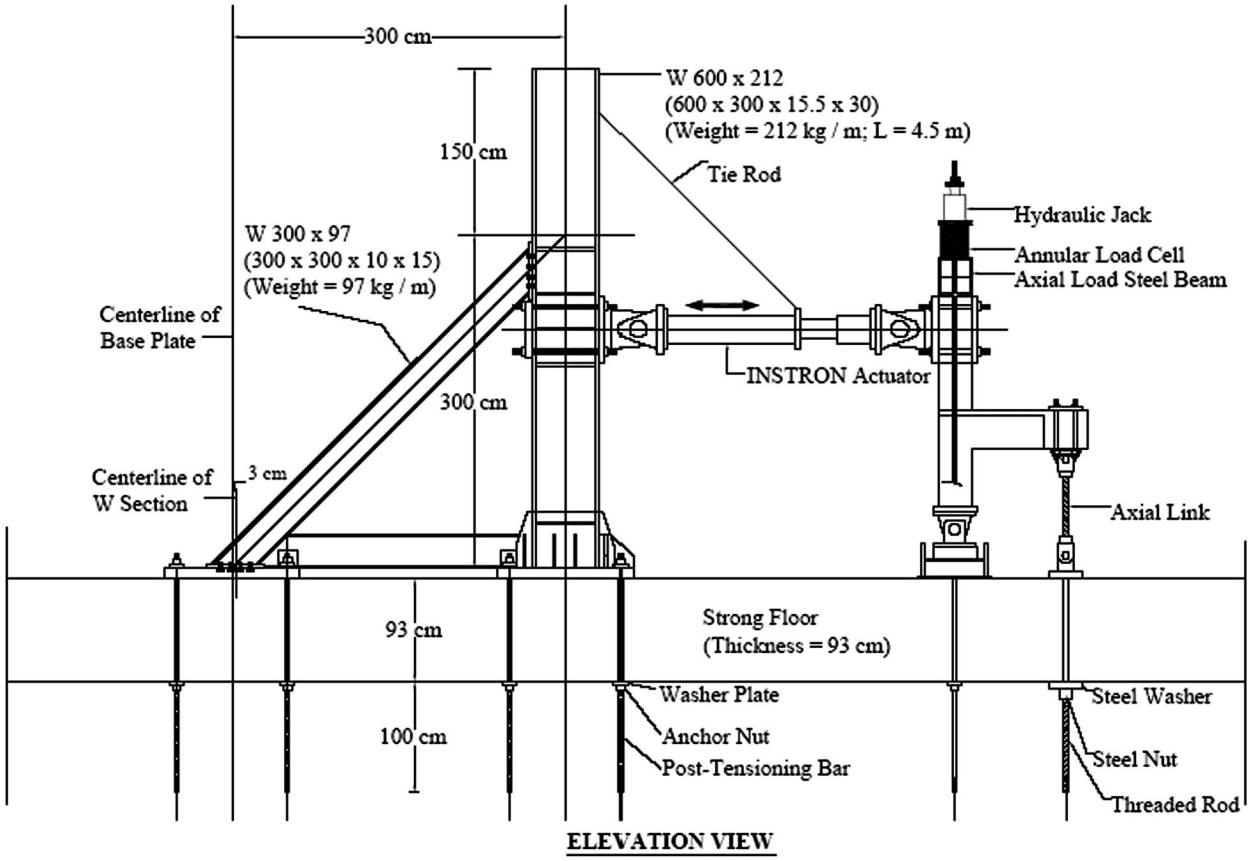

Fig. 9. Schematic diagram (elevation) of the test setup designed for testing of joints

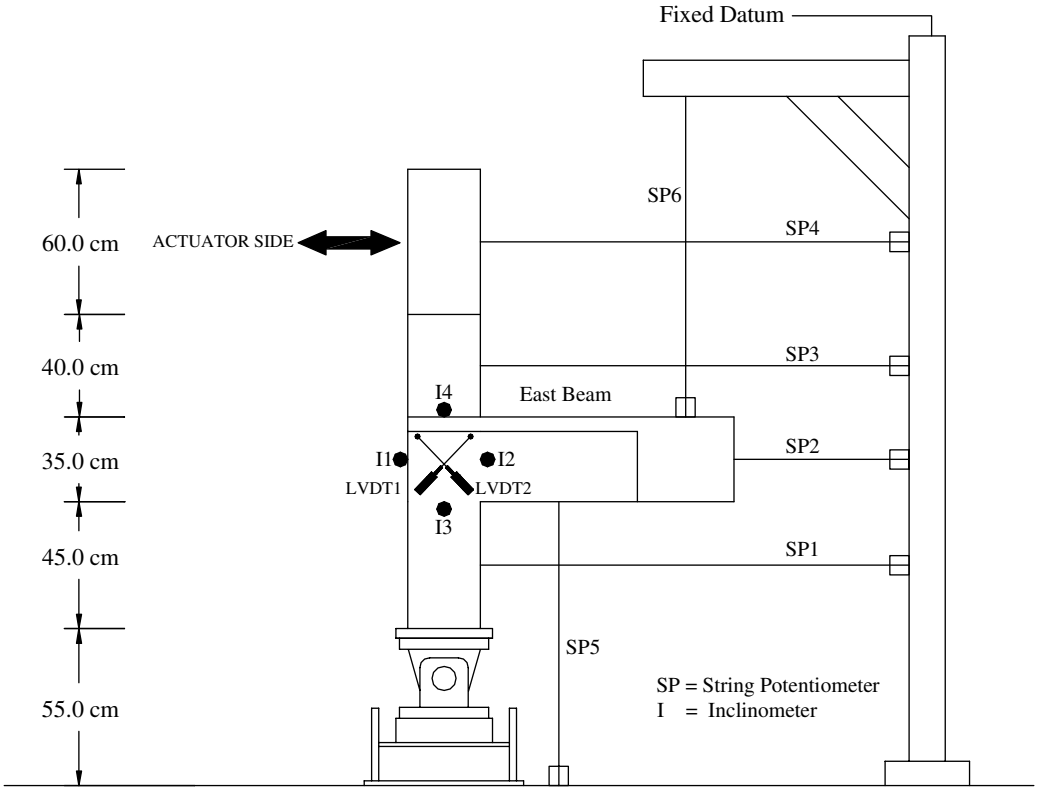

Fig. 10. Instrumentation layout for test specimens

Downloaded 01 Apr 2012 to 212.138.47.15. Redistribution subject to ASCE license or copyright. Visit http://www.ascelibrary.org

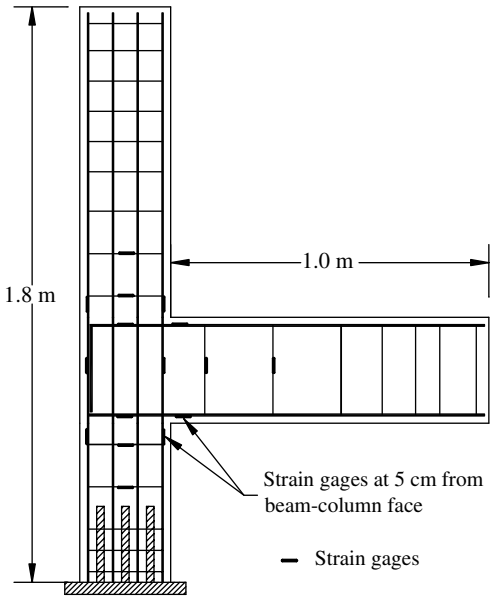

Fig. 11. Layout of strain gages in the as-built test specimen

Testing Procedure

The horizontal-loading regime was based on the conventional guidelines of quasi-static type testing as followed by most researchers in simulating seismic forces to test reinforced concrete structures (Karayannis and Sirkelis 2008; Tsonos 2008). The loading cycles were controlled by the peak displacement until failure. For each displacement level (i.e., for a constant value of displacement), three fully reversed cycles were completed. The lateral displacement time histories of the experiment are shown in Figs. 12–16. All cycles were started with the pull direction first, then went into the push direction.

Discussion of Test Results

In the present section, through various experimental results, the effectiveness of FRP and/or TRM in improving the as-built joint shear strength and ductility has been studied.

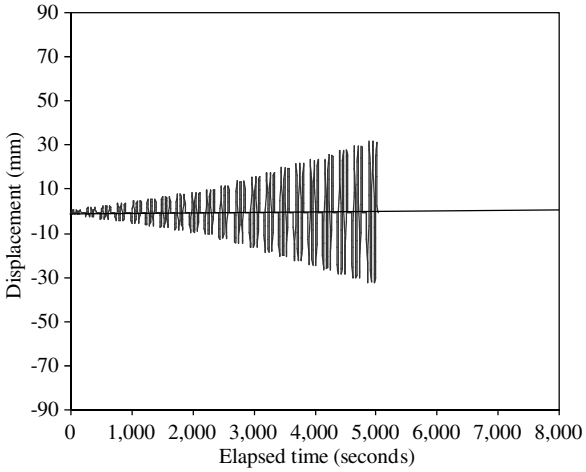

Fig. 12. Displacement time history for as-built control specimen ECON1

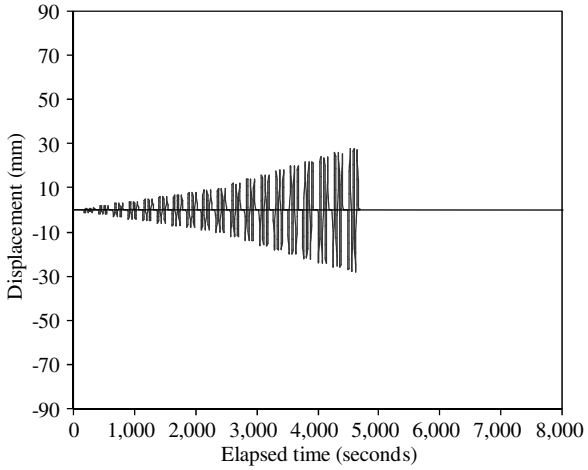

Fig. 13. Displacement time history for as-built control specimen ECON2

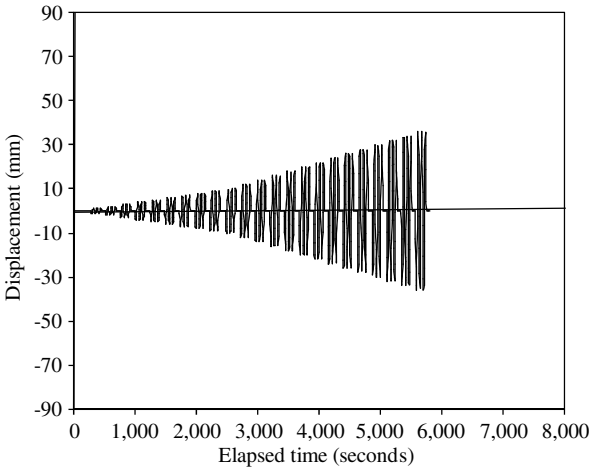

Fig. 14. Displacement time history for CFRP-strengthened specimen ECFRP

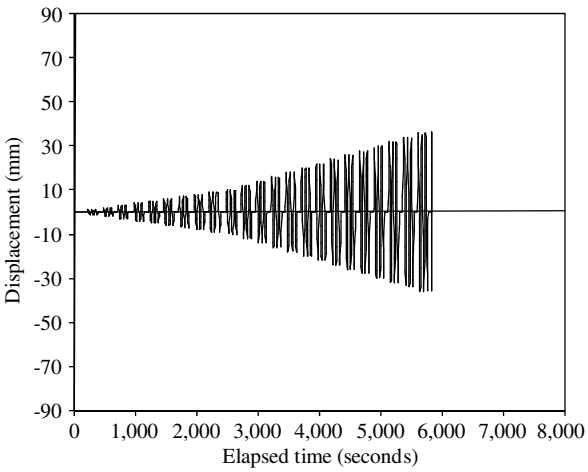

Fig. 15. Displacement time history for GFRP-strengthened specimen EGFRP

Downloaded 01 Apr 2012 to 212.138.47.15. Redistribution subject to ASCE license or copyright. Visit http://www.ascelibrary.org

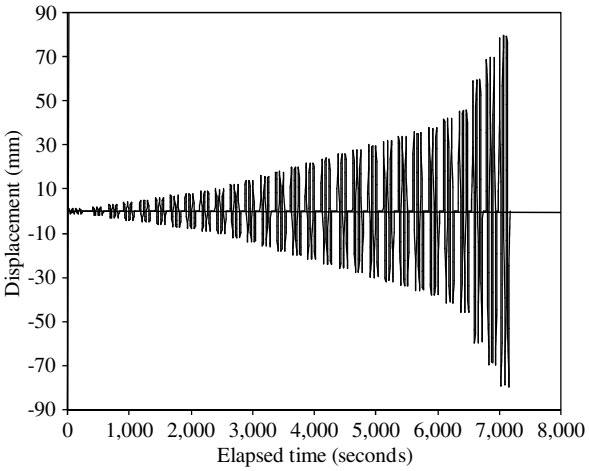

Fig. 16. Displacement time history for TRM-strengthened specimen ECTRM

Fig. 17 shows the general response of joint specimens under lateral cyclic loading. Fig. 17 shows the failure pattern of the control specimen. The figure shows that during the displacement controlled loading stages, significant *X*-shear cracks appeared in the specimen almost symmetrically on both faces of the joint. The shear cracks initiated in diagonal directions and propagated toward the ends of joint. This may be attributed to diagonal tension caused because of excessive shear stresses in the joint. For the TRM-strengthened beam the development of cracks in the specimen during testing was carefully observed, and significant cracks were marked on the specimen itself. Nearly at 6 mm of displacement, few cracks, almost vertical, appeared in the slab region because of significant flexural stresses in the flange of the beam. Further displacement caused the development of cracks in the midspan region of the beam. These cracks were also almost vertical, indicating excessive flexural stresses in the beam attributed to a substantial bending moment in the beam. After further increment of the loads, cracks started appearing in the TRM of joint region. The cracks were significantly inclined, which may be attributed to development of high shear stress in the joint region at higher stages of loading. These shear cracks appeared much later than control

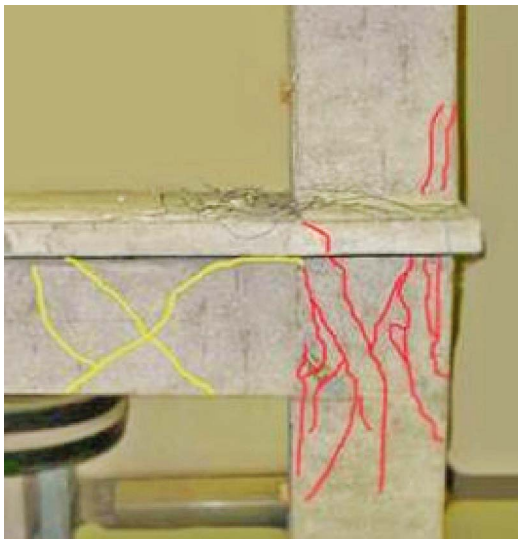

Fig. 17. Cracking pattern of the as-built control specimen (image by the authors)

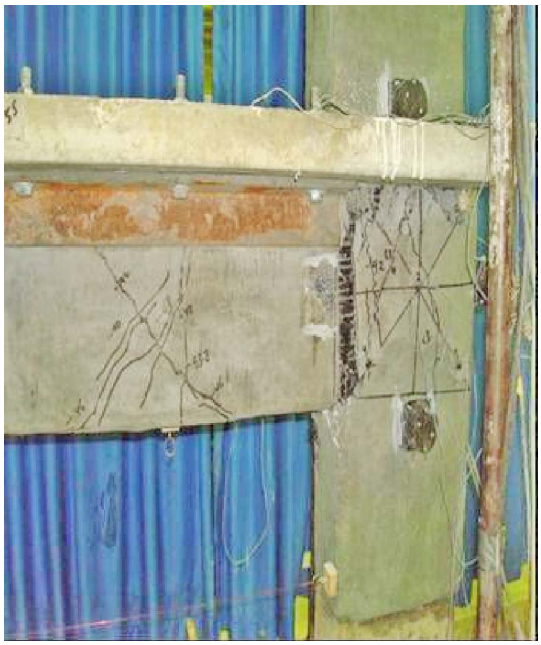

Fig. 18. Failure pattern of TRM-strengthened specimen (image by the authors)

specimens. This indicates the delay of shear cracks by using TRM-strengthening. At about 40 mm displacement, the excessive shear cracks were seen in the joint region, and the load reached its peak value (53 kN). The load started dropping down after this displacement, indicating sufficient degradation of stiffness of the specimen. At approximately a 20% drop in the peak lateral load, the specimen showed substantial cracks in the joint, at the beam-joint interface and at the interface of slab and columns (Fig. 18). The fracture of the textile fibers was also observed at higher stages of loading. The fibers started breaking near the bottom of the beam-column joint interface at higher stages of loading. The fracture of fibers continued in a vertical upward direction until the last textile fiber was broken.

The CFRP-strengthened specimen showed a similar behavior to the one mentioned in Al-Salloum et al. (2011). As debonding was not prevented, the failure was primarily because of debonding of

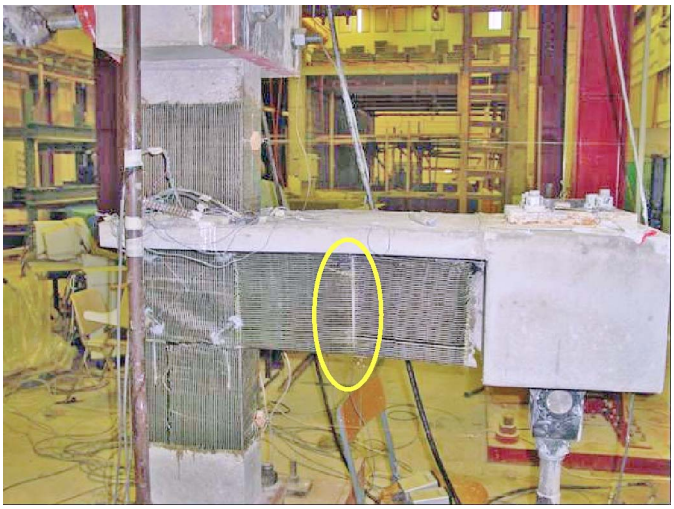

Fig. 19. Failure pattern of CFRP-strengthened specimen (image by the authors)

Downloaded 01 Apr 2012 to 212.138.47.15. Redistribution subject to ASCE license or copyright. Visit http://www.ascelibrary.org

CFRP sheets in the beam region. Tearing of the CFRP sheet was also observed in the beam region because of the fact that at higher stages of loading, there was significant yielding in beam reinforcing bars that allowed cracks to widen in the beam region, which in turn ultimately tore the CFRP sheets (Fig. 19). In the case of GFRP strengthening, debonding was not observed because the sheets were prevented against debonding through a mechanical anchorage system. Because of the prevention of debonding, at higher stages of loading, tearing of GFRP sheets was observed (Fig. 20). The number of layers used in GFRP strengthening was two, whereas number of layers in CFRP-strengthening was only one. It is for reason that similar peak loads were observed with GFRP and CFRP strengthening.

Hysteretic Behavior

The hysteretic behavior of exterior joints was examined in terms of shear strength (measured in ultimate load) and deformation capacity. The load-displacement relationships for control and strengthened specimens are shown as hysteretic curves in Figs. 21–25. Figs. 21 and 22 show that for control specimens, deformability is very poor as specimens reach to their ultimate load at a displacement of 26 mm. On the other hand, CFRP strengthening provides a higher load-carrying capacity than control, GFRP-strengthened, and TRM-strengthened specimens. However, deformability of CFRP strengthening is not as good as GFRP or TRM strengthening (Figs. 23 and 24). This suggests that the use of TRM and GFRP is preferable over CFRP strengthening under seismic excitations because of better deformability of GFRP- and TRM-strengthened joints. Deformability and ductility are important requirements for RC structural components to survive during seismic excitations. The ultimate load for strengthened specimens is higher than control specimens. This is primarily because of the increased confinement of the joint, resulting from externally bonded FRP sheets or a TRM textile system. Also, the hysteretic loops of specimens showed considerable pinching and continuous stiffness degradation with increasing displacement. The loss of stiffness was primarily

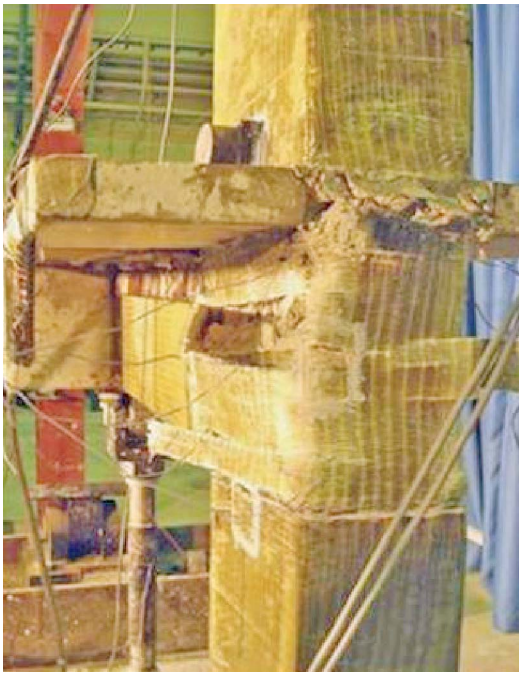

Fig. 20. Failure pattern of GFRP-strengthened specimen (image by the authors)

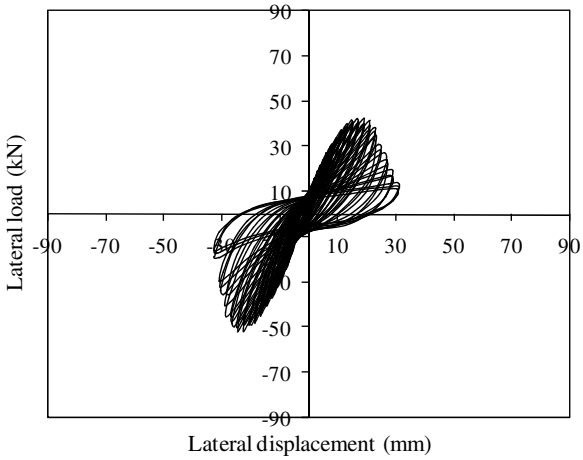

Fig. 21. Load-displacement hysteretic curves for as-built control specimen (ECON1)

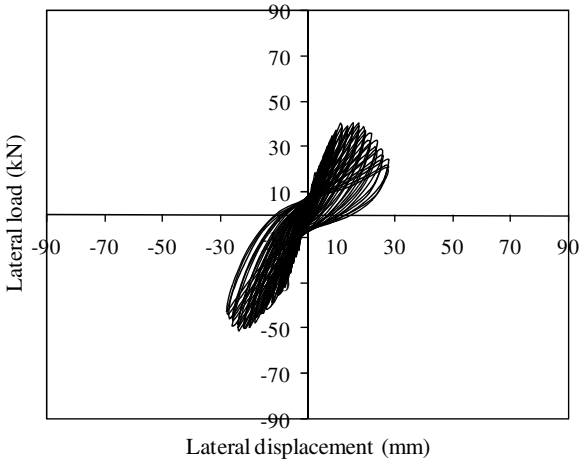

Fig. 22. Load-displacement hysteretic curves for as-built control specimen (ECON2)

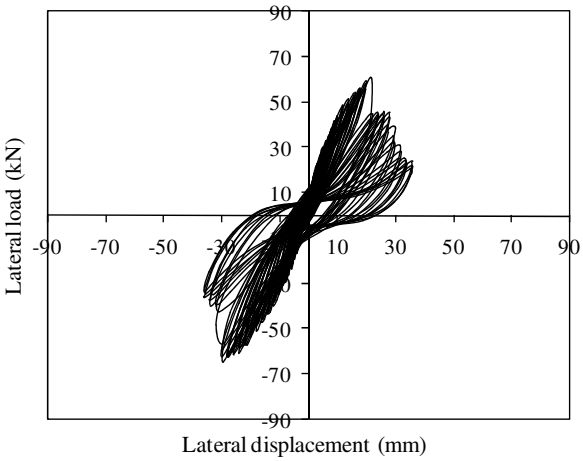

Fig. 23. Load-displacement hysteretic curves for CFRP-strengthened specimen (ECFRP)

Downloaded 01 Apr 2012 to 212.138.47.15. Redistribution subject to ASCE license or copyright. Visit http://www.ascelibrary.org

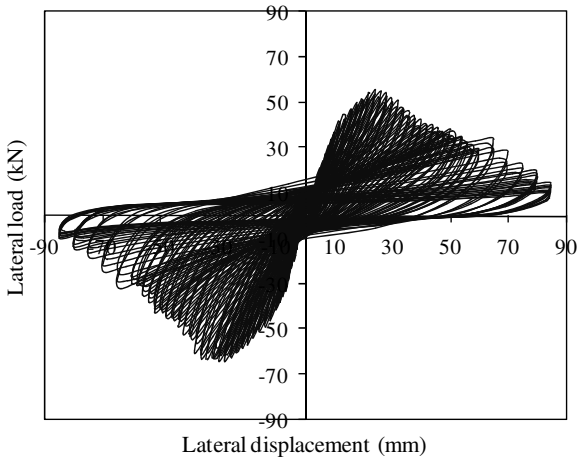

Fig. 24. Load-displacement hysteretic curves for GFRP-strengthened specimen (EGFRP)

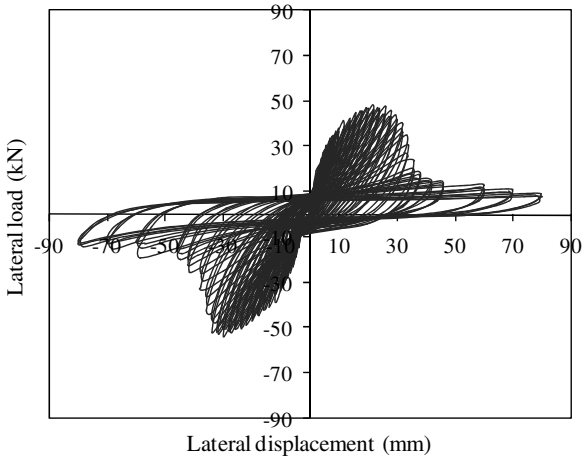

Fig. 25. Load-displacement hysteretic curves for TRM-strengthened specimen (ETRM)

attributed to concrete deterioration in the beam-column joint region. The pinching of the hysteretic loops for cycles after the yielding of the beam's longitudinal reinforcement indicates that the stiffness is fairly low near the zero displacement point in these cycles because the cracks did not close.

Load-Displacement Envelope

To study the load-carrying capacity and ductility of control and strengthened exterior joint specimens, envelopes of load-displacement hysteretic curves were plotted (Fig. 26) and by using these envelopes the peak load, ultimate displacements, ductility, joint shear strength, and diagonal tension for the specimens were obtained and listed in Table 4. The second column of Table 4 shows the average peak load (i.e., average of peak push and pull values), and the third column shows the displacement corresponding to the first yield of steel bars. This displacement is required to calculate ductility of the specimens. The estimated ductility, an important parameter for earthquake-resistant members, is shown in the fourth column of Table 4. The ductility is computed as the ratio of ultimate displacement to the displacement at the first yield of internal steel. For computation, the ultimate displacement was set at a displacement corresponding to 20% drops of the peak load (Δ_{20}). Because there is no well-defined

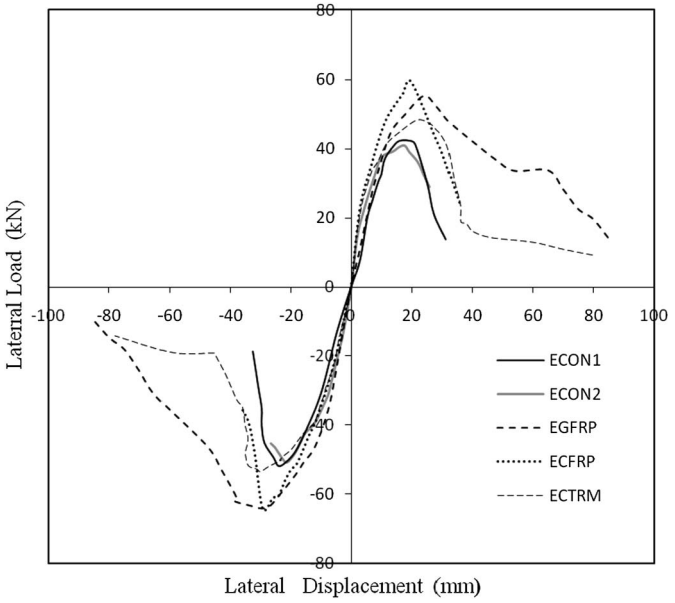

Fig. 26. Envelopes of hysteretic plots for as-built control and strengthened specimens

yield point for the RC beam-column joint specimens, the yield displacement was found by drawing a line between the origin and the 50% load capacity point of the load-displacement envelope. This line was extended to intersect the 80% load capacity horizontal line. The displacement corresponding to the intersection point was assumed as the ultimate displacement.

The values of ductility clearly show that the application of FRP sheets and TRM has improved the ductility of the strengthened specimen significantly. The first column of Table 5 indicates that the increase in strength attributed to CFRP strengthening is the maximum and attributed to TRM, it is the minimum. GFRP sheets, however, increase the strength more than TRM but less than CFRP sheets. This trend is very well expected because fibers of carbon are the strongest and textile-fibers are the weakest. The trend may be altered by changing the governing parameters e.g., the number of layers. The ductility is also substantially increased because of strengthening, and it is the maximum for GFRP-strengthened sheets.

Fig. 26 shows that in the push direction, the contribution of GFRP sheets to strength is more than CFRP sheets, whereas in the pull direction CFRP sheets provide better strength than GFRP sheets. This may be attributed to different stiffness of the strengthened specimens in push and pull directions. The CFRP-strengthened specimen had more stiffness than the GFRP-strengthened specimen in the pull direction, whereas the two-layered GFRP-strengthened specimen had more stiffness in the push direction. It is for this reason that Fig. 26 shows a higher peak load for GFRP-strengthened specimens in the push direction than the CFRP-sheeted specimen. The TRM-strengthened specimen shows lower peak loads than CFRP or GFRP sheeted specimens in both directions (i.e., push and pull directions).

The peak load and deformation capacity of FRP- or TRM-strengthened specimens are very much dependent on the number of layers used in the upgrading. It is possible to increase the strength of strengthened specimens further with the use of more numbers of layers. However, before increasing the number of layers it is essential to make sure that (1) change in the stiffness of the system (attributed to the increased number of layers) does not adversely affect the load sharing between the members and (2) does

Downloaded 01 Apr 2012 to 212.138.47.15. Redistribution subject to ASCE license or copyright. Visit http://www.ascelibrary.org

Table 4. Peak Test Load and Maximum Ductility

Specimen	Peak load (Average) kN	Displacement at first yield of steel, Δ_y (mm)	Ultimate displacement after 20% drop in peak load Δ_{20} (mm)	Ductility Factor Δ_{20}/Δ_y	Shear strength in $\gamma\sqrt{f'_c}$ (MPa)	Diagonal tension (MPa)
ECNO1	47.1	15.7	26.6	1.69	$0.78\sqrt{f'_c}$	2.43
ECNO2	45.81	13.91	25	1.82	$0.79\sqrt{f'_c}$	2.46
ECFRP	61.82	12.44	35	2.89	$1.04\sqrt{f'_c}$	3.69
EGFRP	59.71	12.11	41	3.36	$1.01\sqrt{f'_c}$	3.56
ECTRM	50.88	11.54	33	2.84	$0.85\sqrt{f'_c}$	2.77

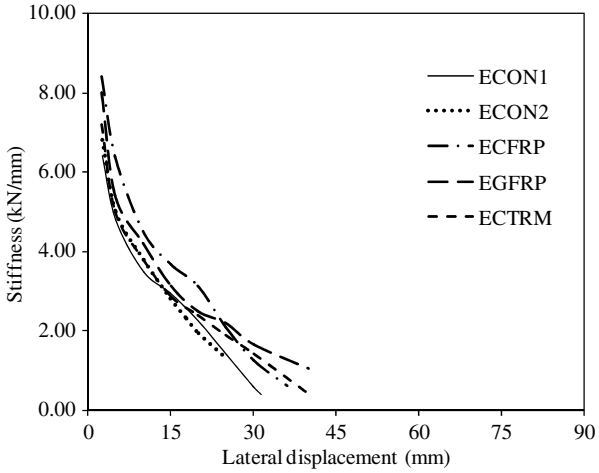

Fig. 27. Stiffness degradation in as-built control and strengthened specimens

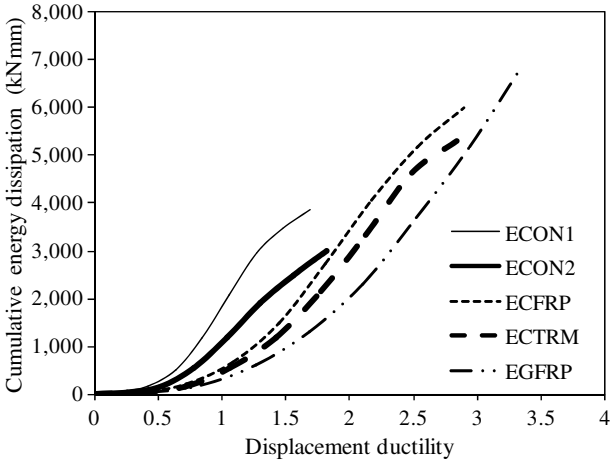

Fig. 28. Cumulative energy dissipation by the control and strengthened specimens

not result in early debonding, if not prevented against debonding, without development of FRP strength.

Stiffness Degradation

The beam-column joint stiffness was approximated as the slope of the peak-to-peak line in each loop. Fig. 27 shows the stiffness degradation with lateral displacement. This degradation may be attributed to concrete nonlinear deformations, flexural and shear cracking, distortion of the joint panel, slippage of reinforcement, loss of cover, and debonding or delamination of FRP. A comparison of the strengthened specimens curve with the corresponding control specimen curve shows that the initial stiffness of the strengthened specimens are significantly higher than that of their corresponding control specimen. This higher initial stiffness for the strengthened specimen may be attributed to the external bonding of FRP sheets or TRM layers on beams, joint, and column regions. The use of FRP or TRM shows that the degradation in the stiffness is slow compared to control specimens. The slow degradation is a desirable property in earthquake-like situations. It was observed in the past earthquakes that most of the RC structures failed (or collapsed) because of a sudden loss of stiffness of the structural joints with increasing lateral movement of the structure.

Energy Dissipation

The area enclosed by a hysteretic loop at a given cycle represents the energy dissipated by the specimen during this cycle. The capability of a structure to dissipate energy has a strong influence on its response to an earthquake loading. The total energy dissipated by a structure consists of (1) energy dissipated by the steel reinforcement, (2) energy dissipated by friction along existing cracks in concrete, and (3) energy dissipated during the formation of new cracks (El-Amoury and Ghobarah 2002). Fig. 28 shows the cumulative energy dissipated by the five specimens. The peak value of each curve presents the cumulative values of full energy dissipation for each tested specimen. Full energy dissipation is an indication of the maximum capacity of the specimen to be stressed until failure. For control specimens, the energy dissipation was relatively low. This is clear from the small areas enclosed by the hysteresis loops seen in previous hysteretic curves. The energy dissipation for strengthened specimens was much larger than that for reference specimens. This is obvious from the large areas enclosed by the hysteresis loops seen in previous figures. Fig. 28 clearly illustrates that the energy dissipation ability of strengthened specimens are substantially higher than that of as-built beam-column joint specimens. The curves also indicate that the energy dissipation ability of a TRM-strengthened specimen is comparable to that of FRP-strengthened specimens.

Conclusions

In the present study, effectiveness of TRM in improving the load-carrying capacity and ductility of a shear deficient exterior joint was studied, and its performance was compared with specimens strengthened by using FRP sheets. The following are the major conclusions that can be drawn from the present experimental study:

- The TRM can effectively improve both the shear strength and ductility of seismically deficient beam-column joints to that extent that is comparable to FRP-upgraded joints.

Downloaded 01 Apr 2012 to 212.138.47.15. Redistribution subject to ASCE license or copyright. Visit http://www.ascelibrary.org

- The increase in peak load and ductility by TRM upgrading is very much dependent on the number of layers used in the strengthening. It is possible for TRM-upgraded specimen to achieve comparable FRP-upgraded beam-column joint ultimate load values with the use of a sufficient number of layers.
- Before increasing the number of TRM or FRP layers it is essential to make sure that (1) change in the stiffness of the system (because of increased number of layers) does not adversely affect the load sharing between the members and (2) does not result in early debonding if not prevented through mechanical anchorages.
- The energy dissipation ability of the TRM-strengthened beam-column joint is substantially higher than that of an as-built beam-column joint and comparable to FRP-upgraded joints.

Acknowledgments

The writers gratefully acknowledge the support provided by the *Specialty Units for Safety and Preservation of Structures* and the *MMB Chair for Research and Studies in Strengthening and Rehabilitation of Structures* at the Department of Civil Engineering, King Saud University.

References

Al-Jamous, A., Ortlepp, R., Ortlepp, S., and Curbach, M. (2006). "Experimental investigations about construction members strengthened with textile reinforcement." *Proc., 1st Int. Conf. on Textile Reinforced Concrete (ICTRC'2006)*, J. Hegger, W. Brameshuber, and N. Will, eds., Institute of Concrete Structures, RILEM Publications SARL, TU Dresden, Germany, 161–170.

Almusallam, T. H., and Al-Salloum, Y. A. (2007). "Seismic response of interior beam-column joints upgraded with FRP sheets. II: Analysis and parametric study." *J. Compos. Constr.*, 11(6), 590–600.

Al-Salloum, Y. A., and Almusallam, T. H. (2007). "Seismic response of interior beam-column joints upgraded with FRP sheets. I: Experimental study." *J. Compos. Constr.*, 11(6), 575–589.

Al-Salloum, Y. A., Almusallam, T. H., Alsayed, S. H., and Siddiqui, N. A. (2011). "Seismic behavior of as-built, ACI-complying and CFRP-repaired exterior RC beam-column joints." *J. Compos. Constr.*, 15(4), 522–534.

Alsayed, S. H., Almusallam, T. H., Al-Salloum, Y. A., and Siddiqui, N. A. (2010a). "Seismic rehabilitation of corner RC beam-column joints using CFRP composites." *J. Compos. Constr.*, 14(6), 681–692.

Alsayed, S. H., Al-Salloum, Y. A., Almusallam, T. H., and Siddiqui, N. A. (2010b). "Seismic response of FRP-upgraded exterior RC beam-column joints." *J. Compos. Constr.*, 14(2), 195–208.

Antonopoulos, C., and Triantafillou, T. C. (2003). "Experimental investigation of FRP-strengthened RC beam-column joints." *J. Compos. Constr.*, 7(1), 39–49.

Antonpoulos, C. P., and Trantfillou, T. C. (2002). "Analysis of FRP-strengthened beam-column joints." *J. Compos. Constr.*, 6(1), 41–51.

ASTM. (1985). "Method for tensile strength of hydraulic cement mortars." *C190-85*, West Conshohocken, PA.

ASTM. (2002). "Standard test method for compressive strength of hydraulic cement mortars (Using 2-in. or [50-mm] Cube Specimens)." *C109/C109M-02*, *Annual book of ASTM standards*, Vol. 4.01, West Conshohocken, PA.

ASTM. (2011). "Standard test methods and definitions for mechanical testing of steel products." *A370-11*, West Conshohocken, PA.

Balsamo, A., Colombo, A., Manfredi, G., Negro, P., and Prota, A. (2005). "Seismic behavior of a full-scale RC frame repaired using CFRP laminates." *Eng. Struct.*, 27(5), 769–780.

Basalo, F. J. D., Matta, F., and Nanni, A. (2009). "Fiber reinforced cementitious matrix composites for infrastructure rehabilitation." *Composites & Polycon 2009*, American Composites Manufacturers Association, Tampa FL.

Di Ludovico, M., Prota, A., Manfredi, G., and Cosenza, E. (2008). "Seismic strengthening of an under-designed RC structure with FRP." *Earthquake Eng. Struct. Dyn.*, 37(1), 141–162.

El-Amoury, T., and Ghobarah, A. (2002). "Seismic rehabilitation of beam-column joint using GFRP sheets." *Eng. Struct.*, 24(11), 1397–1407.

Engindeniz, M., Kahn, L. F., and Zureick, A. (2008a). "Performance of an RC corner beam-column joint severely damaged under bi-directional loading and rehabilitated with FRP composites." *SP-258: Seismic Strengthening of Concrete Buildings Using FRP Composites* (CD-ROM), T. Alkhrdahi, and P. Silva, eds., American Concrete Institute, Farmington Hills, MI, pp. 148.

Engindeniz, M., Kahn, L. F., and Zureick, A. (2008b). "Pre-1970 RC corner beam-column-slab joints: seismic adequacy and upgradability with CFRP composites." *Proc., 14th World Conf. on Earthquake Engineering*, China Earthquake Administration Ministry of Construction, Beijing, 12–17.

Gergely, J., Pantelides, C. P., and Reaveley, L. D. (2000). "Shear strengthening of RCT-joints using CFRP composites." *J. Compos. Constr.*, 4(2), 56–64.

Ghobarah, A., and El-Amoury, T. (2005). "Seismic rehabilitation of deficient exterior concrete frame joints." *J. Compos. Constr.*, 9(5), 408–416.

Ghobarah, A., and Said, A. (2001). "Seismic rehabilitation of beam-column joints using FRP laminates." *J. Earthquake Eng.*, 5(1), 113–129.

Ghobarah, A., and Said, A. (2002). "Shear strengthening of beam-column joints." *Eng. Struct.*, 24(7), 881–888.

Karayannis, C., and Sirkelis, G. (2008). "Strengthening and rehabilitation of RC beam-column joints using carbon-FRP jacketing and epoxy resin injection." *J. Earthquake Eng. Struct. Dyn.*, 37(5), 769–790.

Kurtz, S., and Balaguru, P. (2001). "Comparison of inorganic and organic matrices for strengthening of RC beams with carbon sheets." *J. Struct. Eng.*, 127(1), 35–42.

Lee, W. T., Chiou, Y. J., and Shih, M. H. (2010). "Reinforced concrete beam-column joint strengthened with carbon fiber reinforced polymer." *Compos. Struct.*, 92(1), 48–60.

Mukherjee, A., and Joshi, M. (2005). "FRPC reinforced concrete beam-column joints under cyclic excitation." *Compos. Struct.*, 70(2), 185–199.

Pampanin, S., Bolognini, D., and Pavese, A. (2007). "Performance-based seismic retrofit strategy for existing reinforced concrete frame systems using fiber-reinforced polymer composites." *J. Compos. Constr.*, 11(2), 211–226.

Pantelides, C. P., Okahashi, Y., and Reaveley, L. D. (2008). "Seismic rehabilitation of reinforced concrete frame interior beam-column joints with FRP composites." *J. Compos. Constr.*, 12(4), 435–445.

Papanicolaou, C. G., Triantafillou, T. C., Karlos, K., and Papathanasiou, M. (2007). "Textile-reinforced mortar (TRM) versus FRP as strengthening material of URM walls: In-plane cyclic loading." *Mater. Struct.*, 40(10), 1081–1097.

Triantafillou, T. C., and Papanicolaou, C. G. (2005). "Textile reinforced mortars (TRM) as strengthening materials of concrete structures." *Proc., fib Symposium "Keep Concrete Attractive"*, G. L. Balazs, and A. Borosnyoi, eds., Hungarian Group of fib, Budapest, Hungary, 345–350.

Triantafillou, T. C., and Papanicolaou, C. G. (2006). "Shear strengthening of reinforced concrete members with textile reinforced mortar (TRM) jackets." *Mater. Struct.*, 39(1), 93–103.

Triantafillou, T. C., Papanicolaou, C. G., Zissimopoulos, P., and Laourdekis, T. (2006). "Concrete confinement with textile-reinforced mortar jackets." *ACI Struct. J.*, 103(1), 28–37.

Tsonos, A. (2008). "Effectiveness of CFRP-Jackets and RC-Jackets in post-earthquake and pre-earthquake retrofitting of beam-column subassemblages." *Eng. Struct.*, 30(3), 777–793.

Tsonos, A. (2010). "Performance enhancement of R/C building columns and beam-column joints through shotcrete jacketing." *Eng. Struct.*, 32(3), 726–740.

Wu, H. C., and Sun, P. (2005). "Fiber reinforced cement based composite sheets for structural retrofit." *Proc., Int. Symp. on Bond Behavior of FRP in Structures (BBFS)*, Hong Kong, China.

Downloaded 01 Apr 2012 to 212.138.47.15. Redistribution subject to ASCE license or copyright. Visit http://www.ascelibrary.org